Two-Step Polarization Switching in Ferroelectric Polymers

Yangjiang Wu,[1,2,3] Xiaohui Li,[1,2,3] Alain M. Jonas,[4] and Zhijun Hu[1,2,3,*]

[1]Center for Soft Condensed Matter Physics and Interdisciplinary Research & Collaborative Innovation Center of Suzhou Nano Science and Technology, Soochow University, Suzhou 215006, China

[2]Jiangsu Key Lab of Advanced Optical Manufacturing Technologies, College of Physics, Optoelectronics and Energy, Soochow University, Suzhou 215006, China

[3]Research Center for Functional Organic/Polymer Micro/Nanofabrication, College of Materials, Chemical and Chemical engineering, Soochow University, Suzhou 215123, China

[4]Institute of Condensed Matter and Nanosciences—Bio & Soft Matter (IMCN/BSMA), Université catholique de Louvain, Croix du Sud 1/L7.04.02, B-1348 Louvain-la-Neuve, Belgium

(Received 11 June 2015; revised manuscript received 14 October 2015; published 23 December 2015)

The correlation between hierarchical structures and polarization switching in ferroelectric poly (vinylidene fluoride-ran-trifluoroethylene) has been probed by combining transmission electron microscopy studies with piezoresponse force microscopy observations. Differences are demonstrated between homogeneous and anisotropic thin films with well-defined lamellar orientation, with the later exhibiting quadrangular domain shape and double hysteresis. We propose that the polarization switching within lamella is dominated by domain wall flow motion, while the amorphous components between lamellae impede full polarization switching. The coupling between lamellae is controlled by a creep process. These results and interpretations explain well the seemingly contradicting polarization reversal dynamics reported and offer opportunities to change domain reversal speed by making ferroelectric polymer nanostructures.

DOI: 10.1103/PhysRevLett.115.267601 PACS numbers: 77.80.Fm, 68.55.am, 77.55.-g, 77.84.Jd

Ferroelectric materials have been extensively studied in the past decades because they pave the way to a myriad of electrically controlled devices [1–4]. Understanding the mechanism of polarization switching is critical for the prediction and optimization of ferroelectric devices. In this aim, macroscopic electrical measurements are usually performed on ferroelectric capacitors and analyzed within the phenomenological framework of nucleation and growth theory [5–8]. Recently, real-time studies of polarization switching, e.g., x-ray scattering [9], transmission electron microscopy (TEM) [10], and piezoresponse force microscopy (PFM) [11], have shed new light on the switching dynamics. It was revealed that polarization switching is strongly affected by defects in ferroelectric mediums and interfaces [12]. Domain shape and motion are also strongly affected by the presence of defects which act as pinning centers for moving transformation fronts [8]. The polarity and charge defect directly favors one polarization orientation (random field), whereas strain fields can destabilize the ferroelectric phase and induce transition to the nonferroelectric (random bond) [8,13]. The interplay between the driving force and disorder gives rise to a broad spectrum of domain wall motion dynamics, including reversible vibrations, creep, and sliding [11].

Among ferroelectric materials, organic ferroelectrics such as poly(vinylidene fluoride-*ran*-trifluoroethylene) [P(VDF-TrFE)] are especially attractive owing to their high flexibility, low cost, and ease of production [14–16]. In parallel to the efforts concentrating on the development of nondestructive readout capability in ferroelectric memories [17] and on integration with a wide range of semiconductor systems [18,19], P(VDF-TrFE) represents a model system for exploring fundamentals of organic ferroelectrics [20–22]. It was shown for instance that ferroelectric properties exist in films of only a few monolayers [20]. A peculiar switching behavior characterized by intrinsic switching kinetics has been reported for ultrathin monolayers [21]. In polycrystalline thin films, however, a cold-field switching model was proposed to explain the observed nonthermally activated polarization switching [22]. The main cause of the debate on switching mechanisms results from the presence of defects in polymer thin films. Intrinsic switching does not require heterogeneous nucleation, whereas the cold field switching is mediated by defects. At nanoscale, spatially nonuniform velocity of domain growth has been observed and attributed to defects in chain conformation and molecular packing [23,24]. The fact that defects exist at different structural levels makes the unambiguous determination of the polarization switching mechanism rather challenging.

Apart from the defects in molecular conformation and packing of polymer chains, the polarization switching of ferroelectric polymers should be further complicated by the hierarchical structures of semicrystalline polymers. Semicrystalline polymers like P(VDF-TrFE) typically organizes into crystalline lamellae with folded chains interleaved with amorphous layers [25]. Folded chains are oriented approximately perpendicular to the surface of lamellae. The amorphous interlayers consist of folds, loose loops, tie segments, and dangling ends of the polymer chains. These distinctive characteristics make it very

difficult to clarify the physical nature of polarization switching in P(VDF-TrFE) thin films [14]. Elucidating the nature of polarization switching would, however, not only provide an understanding of the fundamental features of ferroelectric properties in organic materials, but also lead to a more rational optimization of organic ferroelectric devices.

In this work, the issue of how hierarchical structures affect polarization switching is addressed by PFM observations on anisotropic P(VDF-TrFE) thin films with controlled location and orientation of lamellar crystals and amorphous interlayers. For this study, P(VDF-TrFE) (72/28 mol%) thin films were prepared by spin coating on silicon wafer. The thin films were then either thermally annealed at 135 °C or embossed with nanoimprint lithography at the same temperature. A silicon mold bearing nanotrenches was used and thus nanostripes of P(VDF-TrFE) were fabricated on substrates. Because of the different electron density in crystalline and amorphous regions of semicrystalline polymers, the hierarchical structures of free-standing P(VDF-TrFE) thin films and nanostripe arrays can be visualized by TEM. The homogeneous P(VDF-TrFE) thin films are composed of needlelike lamellar crystals (dark regions) and amorphous regions (gray regions) randomly distributed in plane [Fig. 1(a)]. The selected area electron diffraction (SAED) pattern is composed of diffraction rings, suggesting a random orientation of the lamellar crystals in the homogeneous thin films. Previous studies have revealed that the needlelike lamellae in homogeneous P(VDF-TrFE) thin films predominantly take an edge-on orientation; i.e., the c axis (chain axis) of lamellae is parallel to the substrate [18,26]. Contrarily, the lamellae in P(VDF-TrFE) nanostripes are aligned preferentially perpendicular to the nanostripes [Fig. 1(b)]. A close look at the lamellar crystals indicates that they have an elliptical shape. Considering the in-plane x-ray diffraction patterns [27] and combined vertical and horizontal PFM observations [28], the arcs in the SAED pattern obtained from the nanostrips are indexed to both (200) and (110) with the $\{010\}$ plane contacting the substrate. This indicates that the c axis of the P(VDF-TrFE) lamellae is parallel to the nanostripes and substrate, while the a axis is aligned preferentially perpendicular to the nanostripes. The polar b axis is tilted away from the surface normal at 30°. To simplify the description, we illustrate a structural model for the hierarchical structures of P(VDF-TrFE) thin films and nanostripes [Figs. 1(c) and 1(d)]. The molecular chains are preferentially aligned in plane and folds back and forth to form lamellar crystals, while the other parts of the chains constitute the amorphous components. The lamellae and amorphous components in homogeneous thin films randomly distribute on the substrates while the molecular chains are well aligned along nanostripes with the lamellae being regularly separated by amorphous regions.

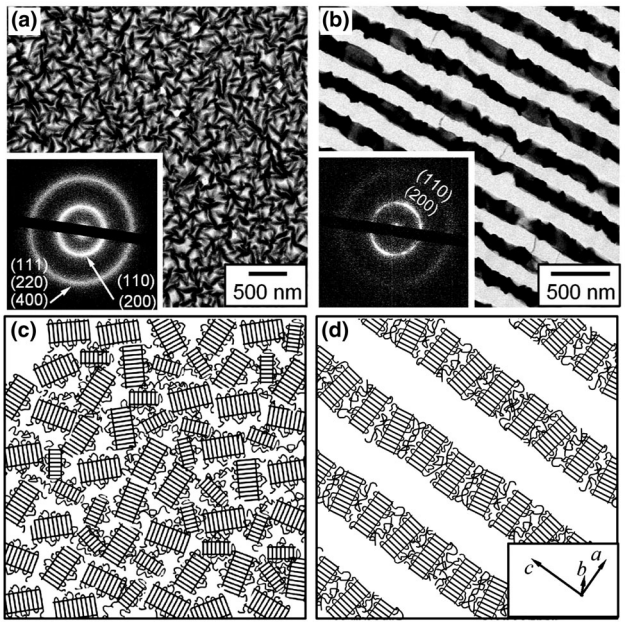

FIG. 1. Hierarchical structures of P(VDF-TrFE) thin films. (a), (b) TEM images of P(VDF-TrFE) homogeneous thin films and nanostripes. The insets are the corresponding SAED patterns. (c), (d) Schematic illustration of the hierarchical structures of P(VDF-TrFE) in homogeneous thin films and nanostripes.

The polarization switching in both homogeneous and anisotropic P(VDF-TrFE) thin films have been generated and visualized using PFM. Figure 2(a) shows a typical topographic image of a 100 nm thick P(VDF-TrFE) thin film. Application of voltage pulses (−8 V, 0.2 s) to the homogeneous thin films results in approximately circular switching domains of about 70 nm radius [Fig. 2(b)]. A close look to the nearly circular domains reveals that their borders are not smooth but rough. Such moderately rough circular domains are consistent with previous observations on P(VDF-TrFE) [23,24] or inorganic ferroelectric thin films [13]. The application of a voltage pulse to the nanostripes with well-oriented lamellae, however, generates reversal domains having a different shape. Figures 2(c) and 2(d) show the simultaneously obtained PFM topography and phase images of 100 nm thick P(VDF-TrFE) nanostripes which are polarized with a voltage pulse of −8 V (0.05–5 s). In contrast to roughly circular domains observed in homogeneous thin films, the reversal domains in nanostripes appear to be nearly rectangular in shape. The long and short sides of the rectangular reversal domains are perpendicular and parallel to the nanostrips, respectively. The anisotropic shape of reversed domains is further evidenced by a process of local polarization switching induced by voltage pulses with incrementally increasing amplitude at a fixed duration (1 s) [Figs. 2(e) and 2(f)].

By taking into account the hierarchical structures of of P (VDF-TrFE) thin films, the different domain shapes in homogeneous thin films and nanostripes can be interpreted as follows. On the molecular level, ferroelectric polarization in the β phase P(VDF-TrFE) arises from the F-C-H dipoles where the main chains take a trans (T) conformation. The T molecular conformation results in the dipoles

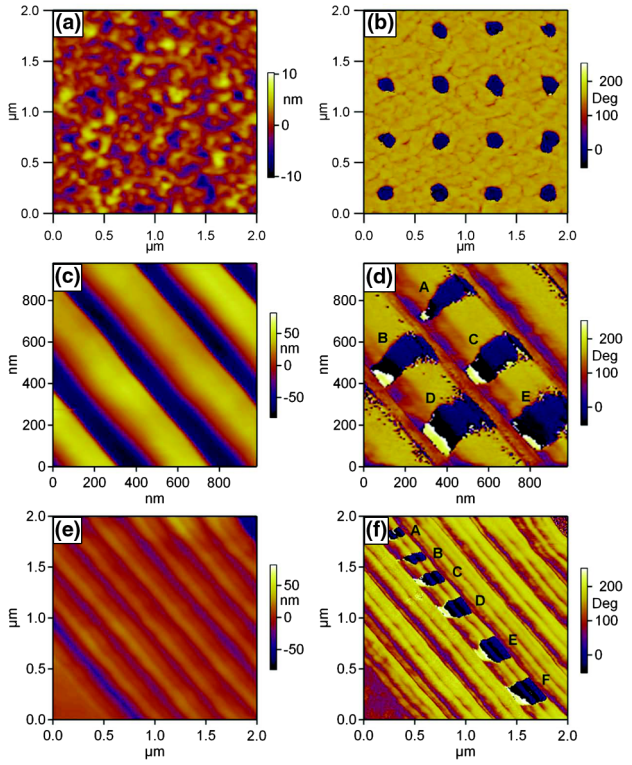

FIG. 2 (color online). PFM topography (a) and PFM phase images (b) of a homogeneous P(VDF-TrFE) thin film. The reversal domains in (b) are generated with a voltage pulse (−8 V, 0.2 s). (c),(d) PFM topography and phase images of P(VDF-TrFE) nanostripes. The reversal domains are generated with voltage pulses (−8 V) of different durations, A ∼0.05, B ∼0.1, C ∼0.5, D ∼1, E ∼5 s. (e) and (f) PFM topography and phase images of P(VDF-TrFE) nanostripes. The dark regions in (f) are reversal domain generated with voltage pulses (1 s) of different amplitude, A ~ -5, B ~ -6, C ~ -7, D ~ -8, E ~ -9, F ~ -10 V.

being oriented perpendicular to the chain axis. The molecular chains pack parallel to each other, forming a crystal lattice with pseudohexagonal quasiorthorhombic symmetry [29]. Taking into account the long chain nature and lattice symmetry of P(VDF-TrFE), a molecular level two-process mechanism of polarization switching has been previously proposed [30]. The first process consists of a rotation of dipoles about the chain axis which is accomplished by the propagation of a kink along the chain direction. The second process involves intermolecular expansion of chain rotations in the $a-b$ plane of crystalline lamellae. The theoretical time needed for kink of rotation along a 10 nm polymer chain lies in the order of picoseconds, which is much shorter than that of the second process [14]. As polymer chains are not infinite in length, the fast domain growth along the c axis of lamellae makes domain walls reach the borders of lamellae in the thickness direction within picoseconds. As a result, patterns of reversal domains in a rectangular shape elongated along the c axis are expected. However, what we observed is that the rectangular domain patterns are elongated along the a axis of lamellae and extend over the nanostripes as soon as they are observed [Figs. 2(c) and 2(e)]. We have tried to shorten the duration of the voltage pulse to be less than 35 ms; however, no reversal domains can be observed from the PFM phase images (Fig. S1 in the Supplemental Material [31]). Once the duration of voltage pulse (−8 V) equals or exceeds 35 ms, completely switched domains elongated perpendicularly to the nanostripes are observed. The minimum width of the reversal domains is about 100 nm, which is much larger than the nominal radius of the PFM tip (∼20 nm). The length of the domains is limited by the width of the nanostripes (∼200 nm). Therefore, it is reasonable to conclude that the velocity of domain growth in the $a-b$ crystal plane is comparable to that along the polymer chains. This indicates that as soon as one nucleation center of a switched domain is formed in the high-field region near the PFM tip, the domain growth will follow the nonactivated process, i.e., domain wall flow motion. This should result from the connectivity of monomers along a polymer chain, the short range van der Waals interactions, and long range dipole-dipole interactions between chains. In the case of homogenous thin films, simultaneous domain nucleation may take place in several lamellae. The complete polarization switching in individual lamellae leads to circular domain patterns with some roughness arising from crystal boundaries. For the nanostripes, the elliptical lamellar crystals tend to be aligned perpendicularly to the nanostripes. Thus, the complete polarization reversal of individual lamellae would result in nearly rectangular domain patterns.

qAs proved and illustrated in Fig. 1, the lamellae are embedded in amorphous interlayers. Previous x-ray and infrared-spectroscopy studies have demonstrated that, in addition to the T conformation, chains occurring in a mixed conformation, TG (gauche) or TG^{-}, are also present in P(VDF-TrFE) [32]. They should be located in the amorphous interlayers. Therefore, after complete polarization switching is accomplished in individual lamella, the domain walls will be pinned by the two-dimensional interfaces between lamellae and amorphous interlayers. However, two neighboring lamellae can be coupled with the in-plane polarization in each lamella. The interlamellae electrostatic coupling would create internal stresses at the interfaces. When amplitude of the applied electric field is higher than a threshold value or the duration is longer than a critical one, the electrostatic coupling process between lamellae will experience a pinning-depinning transition via the chains bridging lamellae. The process should be similar to a creep behavior, which is a consequence of competition between the elastic energy of a propagating interface and a pinning potential preventing it from simply sliding when submitted to an external field [33]. Indeed, as can be seen in Fig. 2 and Fig. S2, the reversal domains propagate successively along the P(VDF-TrFE) nanostripes or logarithmically in homogeneous thin films with increasing the voltage pulse amplitude or duration. This phenomenon

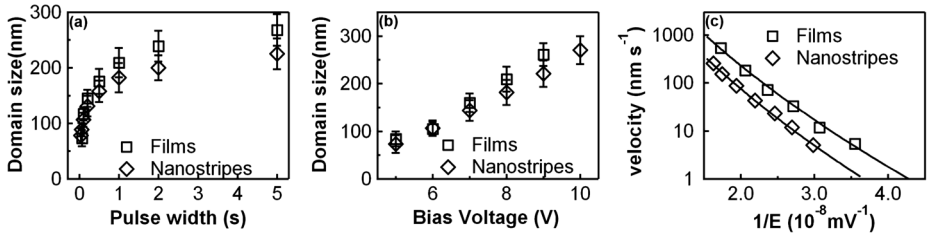

FIG. 3. Statistical data of domain sizes as a function of pulse duration (a) and amplitude (b) in P(VDF-TrFE) homogeneous thin films and nanostripes. (c) The dependence of domain sizes on calculated electric field for thin films and nanostripes. The solid curves were fitted from the data based on Eq. (3).

indicates that the domain growth indeed transforms to creep motion under the spatially decayed electric field applied through the PFM tip.

From the area of the isolated domains, we determined the mean domain sizes in homogeneous thin films and nanostripes. The statistical data as a function of pulse duration and amplitude are presented in Figs. 3(a) and 3(b), respectively. The domain sizes logarithmically depend on voltage pulse duration while they depend linearly on pulse amplitude, consistent with previously reported results on homogeneous thin films [34]. To obtain the electric field distribution, we model the tip as a sphere, with radius R. The relationship between the nonuniform electric field E provided by the PFM tip and space distance r can be approximately expressed as

$$E(r) = \frac{VR}{\sqrt{r^2 + R^2 d}} \tag{1}$$

under a voltage V, where d is the film thickness. The velocity of domain growth

$$v(r) = \frac{r_{n+1} - r_n}{t_{n+1} - t_n} \tag{2}$$

can thus be calculated from the domain sizes with different pulse widths, where the subscript n is a serial number and $r = (r_{n+1} + r_n)/2$. The field-dependent domain growth velocity in both P(VDF-TrFE) nanostripes and homogeneous thin films is presented in Fig. 3(c). The data fit well to a creep formula,

$$v = v_\infty \exp\left(-\frac{E_0}{E}\right)^\mu, \tag{3}$$

with $\mu = 0.5$, where E_0, v_∞, and μ are the threshold electric field, upper limit speed for domain growth, and a dynamical exponent, respectively. The exact dynamic exponent μ is found to be 0.56 and 0.57 for homogeneous thin films and nanostripes. In the creep scenario, the μ depends on both the dimensionality of the system and the nature of the pinning potential. For one-dimensional domain walls $\mu = 0.25$, whereas for two-dimensional ones $\mu = 0.5$ under a pinning potential with a short range [33]. Indeed, $\mu \approx 0.25$ has been observed in one-dimensional P(VDF-TrFE) monolayers [23,24]. The microscopic origin of $\mu = 0.5$ in our case is that the lamellae are much thicker than the monolayer and the resulting interfaces between lamellae and the surrounding amorphous component provide a two-dimensional short range pinning potential.

One assumption made in the creep scenario is that the amorphous components can take part in the polarization switching. This has been justified by the double hysteresis in slowly crystallized P(VDF-TrFE) [35]. To further prove that the amorphous components take part in the polarization switching, we have measured the piezoresponse hysteresis loops over many random places in an individual P(VDF-TrFE) nanostripe and presented it in Fig. 4. Interestingly, the piezoresponse hysteresis loops' curves can be roughly sorted out in two groups with coercive voltages of about ± 2.5 and ± 4.0 V, respectively. Considering the hierarchical structures of P(VDF-TrFE) thin films and the limited radius of curvature of the PFM tip, the repeatable double hysteresis must result from the coexistence of crystalline lamellae and amorphous interlayers, indicating that the amorphous components can take part in the polarization switching of ferroelectric polymers.

In summary, we have elucidated the relationship between hierarchical structures and polarization switching in ferroelectric P(VDF-TrFE) thin films. For homogeneous thin films, the reversal domains are circular in shape due to the random in-plane orientation of lamellae. In nanostripes with well oriented lamellae and amorphous interlayers, anisotropic domains elongated along the crystallographic a axis can be visualized by PFM. The reversal domains are stabilized by the pinning effects of amorphous components that coexist with crystallites. We propose that the polarization switching within P(VDF-TrFE) lamellae is dominated by domain wall flow motion. Increasing the amplitude or duration of voltage pulse, the coupling

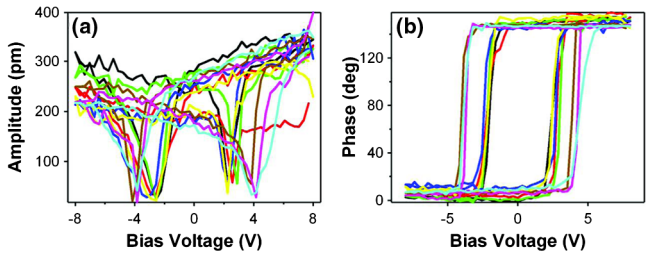

FIG. 4 (color online). (a) PFM amplitude and (b) PFM phase hysteresis loops of an individual P(VDF-TrFE) nanostripe at different locations.

between lamellae propagates via bridging chains at the interfaces between lamellae and surrounding amorphous phase. The coupling between neighboring lamellae can be described with a creep motion model with a dynamic exponent $\mu = 0.5$. The fact that amorphous components take part in the polarization switching is manifested by double local polarization hysteresis.

We note that the two-step polarization switching process can explain very well the recently observed fractal domain patterns in P(VDF-TrFE) thin films [23,24], which should result from domain flow motion within lamellae and pinning of amorphous components at the crystal boundaries. The crossover behavior of frequency-dependent coercivity found in P(VDF-TrFE) [36], can also be interpreted by the two-step model. Finally, we would like to note the applications of these results to technological developments. The electrostatic coupling-driven creep motion of domains across the gap between lamellae implies a strong stability of ferroelectric domains in ferroelectric polymer nanostructures, because the speed of the domain growth becomes exponentially small as the writing voltage goes to zero. Previously, regular arrays of P(VDF-TrFE) nanostructures with densities of 75 Gbit/in^2 have been demonstrated [37]. Further increasing the information storage density is possible by making smaller ferroelectric polymer nanostructures.

We acknowledge support from the National Natural Science Foundation of China (No. 51473112), the National Basis Research Program of China (No. 2012CB821500), a Project of Jiangsu Scientific and Technological Innovation Team (2013), a Project Funded by the Priority Academic Program Development of Jiangsu Higher Education Institutions (PAPD), and the French Community of Belgium (ARC 13/18-052).

*Corresponding author.
zhijun.hu@suda.edu.cn

[1] S. Mathews, R. Ramesh, T. Venkatesan, and J. Benedetto, Science **276**, 238 (1997).
[2] J. F. Scott, Science **315**, 954 (2007).
[3] I. Grinberg, D. V. West, M. Torres, G. Gou, D. M. Stein, L. Wu, G. Chen, E. M. Gallo, A. R. Akbashev, P. K. Davies, J. E. Spanier, and A. M. Rappe, Nature (London) **503**, 509 (2013).
[4] Y. Yuan, T. J. Reece, P. Sharma, S. Poddar, S. Ducharme, A. Gruverman, Y. Yang, and J. Huang, Nat. Mater. **10**, 296 (2011).
[5] M. Avrami, J. Chem. Phys. **8**, 212 (1940).
[6] Y. Ishibashi and Y. Takagi, J. Phys. Soc. Jpn. **31**, 506 (1971).
[7] A. K. Tagantsev, I. Stolichnov, N. Setter, J. S. Cross, and M. Tsukada, Phys. Rev. B **66**, 214109 (2002).
[8] J. Y. Jo, S. M. Yang, T. H. Kim, H. N. Lee, J.-G. Yoon, S. Park, Y. Jo, M. H. Jung, and T. W. Noh, Phys. Rev. Lett. **102**, 045701 (2009).
[9] A. Grigoriev, D.-H. Do, D. M. Kim, C.-B. Eom, B. Adams, E. M. Dufresne, and P. G. Evans, Phys. Rev. Lett. **96**, 187601 (2006).
[10] C. T. Nelson, P. Gao, J. R. Jokisaari, C. Heikes, C. Adamo, A. Melville, S.-H. Baek, C. M. Folkman, B. Winchester, Y. Gu, Y. Liu, K. Zhang, E. Wang, J. Li, L.-Q. Chen, C.-B. Eom, D. G. Schlom, and X. Pan, Science **334**, 968 (2011).
[11] S. V. Kalinin, A. N. Morozovska, L. Q. Chen, and B. J. Rodriguez, Rep. Prog. Phys. **73**, 056502 (2010).
[12] S. M. Yang, J.-G. Yoon, and T. W. Noh, Curr. Appl. Phys. **11**, 1111 (2011).
[13] T. Tybell, P. Paruch, T. Giamarchi, and J.-M. Triscone, Phys. Rev. Lett. **89**, 097601 (2002).
[14] T. Furukawa, Phase Transit. **18**, 143 (1989).
[15] Q.-D. Ling, D.-J. Liaw, C. Zhu, D. S. -H. Chan, E.-T. Kang, and K.-G. Neoh, Prog. Polym. Sci. **33**, 917 (2008).
[16] S. Ducharme and A. Gruverman, Nat. Mater. **8**, 9 (2009).
[17] Z. Hu, M. Tian, B. Nysten, and A. M. Jonas, Nat. Mater. **8**, 62 (2009).
[18] R. C. G. Naber, C. Tanase, P. W. M. Blom, G. H. Gelinck, A. W. Marsman, F. J. Touwslager, S. Setayesh, and D. M. De Leeuw, Nat. Mater. **4**, 243 (2005).
[19] K. Asadi, D. M. De Leeuw, B. De Boer, and P. W. M. Blom, Nat. Mater. **7**, 547 (2008).
[20] A. V. Bune, V. M. Fridkin, S. Ducharme, L. M. Blinov, S. P. Palto, A. V. Sorokin, S. G. Yudin, and A. Zlatkin, Nature (London) **391**, 874 (1998).
[21] S. Ducharme, V. M. Fridkin, A. V. Bune, S. P. Palto, L. M. Blinov, N. N. Petukhova, and S. G. Yudin, Phys. Rev. Lett. **84**, 175 (2000).
[22] I. Stolichnov, P. Maksymovych, E. Mikheev, S. V. Kalinin, A. K. Tagantsev, and N. Setter, Phys. Rev. Lett. **108**, 027603 (2012).
[23] P. Sharma, T. J. Reece, S. Ducharme, and A. Gruverman, Nano Lett. **11**, 1970 (2011).
[24] Z. Xiao, S. Poddar, S. Ducharme, and X. Hong, Appl. Phys. Lett. **103**, 112903 (2013).
[25] B. Wunderlich, *Macromolecular Physics* (Academic Press, New York, 1980).
[26] H. G. Kassa, R. Cai, A. Marrani, B. Nysten, Z. Hu, and A. M. Jonas, Macromolecules **46**, 8569 (2013).
[27] D. Guo and N. Setter, Macromolecules **46**, 1883 (2013).
[28] P. Sharma, D. Wu, S. Poddar, T. J. Reece, S. Ducharme, and A. Gruverman, J. Appl. Phys. **110**, 052010 (2011).
[29] E. Bellet-Amalric and J. F. Legrand, Eur. Phys. J. B **3**, 225 (1998).
[30] Y. Tajitsu, T. Masuda, and T. Furukawa, Jpn. J. Appl. Phys. **26**, 1749 (1987).
[31] See Supplemental Material at http://link.aps.org/supplemental/10.1103/PhysRevLett.115.267601 for the initial polarization switching in P(VDF-TrFE) nanostripes.
[32] V. V. Kochervinskii, Russ. Chem. Rev. **65**, 865 (1996).
[33] P. Chauve, T. Giamarchi, and P. Le Doussal, Phys. Rev. B **62**, 6241 (2000).
[34] Y. Kim, W. Kim, H. Choi, S. Hong, H. Ko, H. Lee, and K. No, Appl. Phys. Lett. **96**, 012908 (2010).
[35] N. Koizumi, Y. Murata, and H. Tsunashima, IEEE Trans. Dielectr. Electr. Insul. **EI-21**, 543 (1986).
[36] W. J. Hu, D.-M. Juo, L. You, J. Wang, Y.-C. Chen, Y.-H. Chu, and T. Wu, Sci. Rep. **4**, 4772 (2014).
[37] X.-Z. Chen, Q. Li, X. Chen, X. Guo, H.-X. Ge, Y. Liu, and Q.-D. Shen, Adv. Funct. Mater. **23**, 3124 (2013).